VOLUME 2, 2018
DOI: 10.31058/j.am.2018.22002

Phase Formation and Electrical Properties of Zinc Titanate Ceramics

Kadiyala Chandra Babu Naidu[1*], Giriyappa Thimmaiah Padma[2], Thota Subba Rao[2], Nagasamudram Suresh Kumar[3], Neelam Raghu Ram[2], Ramesh Singampalli[1], Golla Ranjith Kumar[4], Santa Naresh Kumar[4]

[1] Department of Physics, GITAMDeemed to be University, Bangalore, Karnataka, India
[2] Department of Physics, SK University, Anantapuramu, A.P, India
[3] Department of Physics, JNTUCEA, Anantapuramu, A.P, India
[4] School of Applied Sciences, REVA University, Bangalore, Karnataka, India

Email Address

chandrababu954@gmail.com (K. Chandra Babu Naidu)
*Correspondence: chandrababu954@gmail.com

Received: 15 July 2018**; Accepted:** 30 July 2018; **Published:** 6 August 2018

Abstract:

$ZnTiO_3$ was synthesized by employing the solid state reaction between ZnO and TiO_2 powders mixed in the 1:1 molar ratio. The dielectric properties such as dielectric constant (ε_r) and dielectric loss (tan δ) have been studied in the frequency range 200 Hz to 5MHz by varying the temperature from 40^{o}C to 400^{o}C in steps of 10^{o}C. High value of dielectric constant ~ 50 is observed which can be suitable for high charge storage capacitor applications. The optical properties were also studied using FTIR and UV-Visible Spectra. The band gap was calculated from UV-Visible Spectra.

Keywords:

$ZnTiO_3$, Dielectric Constant (ε_r), Optical Properties, AC-Conductivity

1. Introduction

$ZnTiO_3$ is ofa perovskite type oxide structure and has innumerable number of applications because of its diversified electrical, optical and ferroelectric properties. It has many applications such as microwave resonator [1], gas sensor [2] (for ethanol, NO, CO, etc.), microelectronics [3], metal–air barriers [4], and as high performance catalysts [5, 6] for the complete oxidation of hydrocarbons or CO and NO reduction [7] and paint pigment[8].Commercial electronic systems contain components like capacitors, oscillators and filters. To fabricate these components materials having high dielectric constant, a low dissipation factor, a small temperature coefficient of the resonant frequency (τ_f) or a small temperature coefficient of the dielectric constant (τ_ε) are required. $ZnTiO_3$ shows interesting dielectric properties that makes it a suitable candidate for high performance components. In this paper, we report the structural, dielectric (dielectric constant and dielectric loss), and electrical properties (ac-conductivity properties) of $ZnTiO_3$.

2. Materials and Methods

Initially, the two precursors, 99.5% pure ZnO and TiO_2 (Loba Chemie, India) were mixed in the 1:1 molar ratio.The mixture was grounded for 24 hours and then calcined at 700^{o}C for 12 hours. The powder thus obtained was again grounded for 6 hours. The resulting powder was then pressed into pellets under a pressure of 70 MPa. The pellets were sintered at 800^{o}C for 6 hours. The phase and orientation of bulk ZnTiO3 samples were characterized by X-raydiffractometer (Bruker X-Ray Powder Diffract Meter) using CuKα (λ=1.5407 Å) radiation. The surface morphology was examined by field emission scanning electron microscopy (Hitachi: S-4700), energy dispersive x-ray analyzer (EDAX) (AMETEK system).Absorption spectra had been taken using JASCO UV-Visible spectrophotometer (V-670 PC), FT-IR spectrophotometer (IR affinity-1, Shimadzu). The dielectric measurements at different frequencies were done using HIOKI 3532-50 LCR HiTESTER (Japan). Silver paint was applied on both surfaces of the sample as an ohmic contact. Further, pellet was inserted between the electrodes of the dielectric bridge.

3. Results and Discussion

3.1. Structural Analysis

The diffraction pattern of $ZnTiO_3$ ceramic powder is shown in Fig.1. It can be understood from figure that the observed peaks correspond to rhombohedral perovskite structure. These peaks are in consistent with standard JCPDS file No: 26-1500. These peaks are indexed with miller indices (hkl) and compared with standard JCPDS data as depicted in Fig.1. The maximum intensity of 468 is recorded for (104) plane at a two-theta angle of 32.79^o. This peak attributes lattice parameter of a =b ~5.0791 Å and c ~ 13.916 Å [9] for the present material which is almost in close agreement with JCPDS: 26-1500. Furthermore, the average crystallite size (D) is calculated as 47.9 nm using the Scherer formula [10-13].

$$D = \frac{k\lambda}{\beta \cos\theta} \quad (1)$$

Where, k = 0.9, θ is diffraction angle, λ=0.154056 nm and β is full width half maxima.

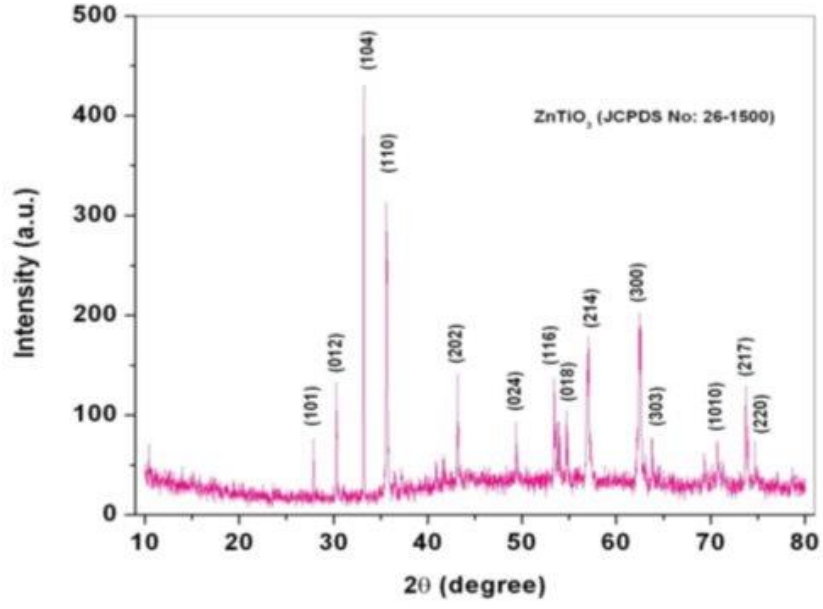

Figure 1. *XRD of $ZnTiO_3$.*

Also, the elastic strain (**ε**~ 0.0015)) is evaluated from a standard relation mentioned elsewhere [14, 15]. The X-ray density(d_x) of ~ 5.174 g/cm^3 is obtained using a formula: ZM/Na^3, where 'Z' is the no. of molecules per unit cell (Z = 1), 'M' is the molecular weight of the composition, 'N' is Avogadro's number (6.023 x 10^{23}) and 'a' is the lattice parameter [16]. Further, the bulk density (d_b)~ 4.654 g/cm^3 is evaluated with the help of Archimedes principle [17]. The pore fraction of (P) is found to be ~ 0.101 by an equation: P~ 1- (d_b/d_x) [18]. The small value of pore fraction establishes a fact that the present material may be of good dense.

3.2. SEM Analysis

The Scanning Electron Microscope (SEM) provides the surface morphology of powder specimen. It is seen from Fig.2 that all the grains are of almost spherical in shape. The average grain size (G_a) is found to be 714 nm using linear intercept method [19].

$$G_a = 1.5L/MN \quad (2)$$

Where L is the test line length, N is the number of intersecting grains and M is the magnification.

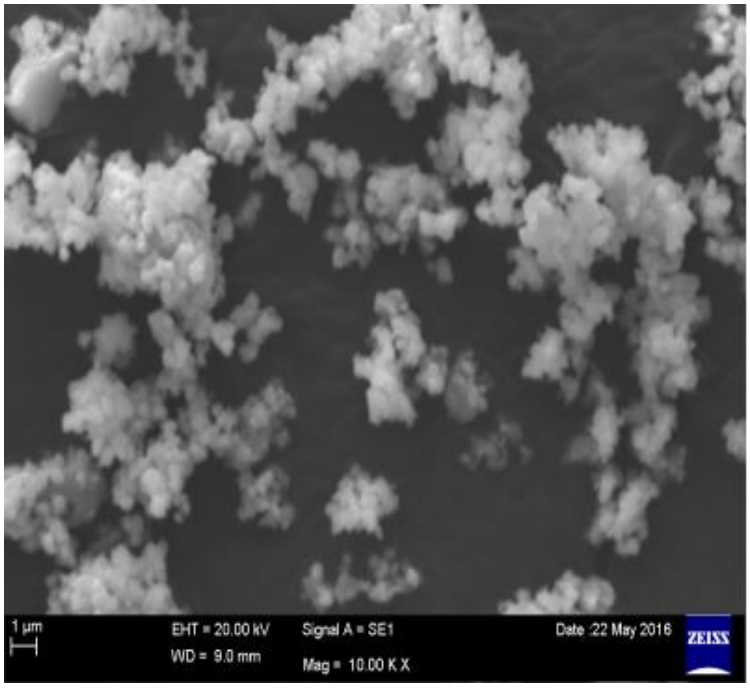

Figure 2. *SEM image of $ZnTiO_3$ ceramic.*

3.3. FTIR Analysis

Fourier Transform Infrared Spectroscopy (FTIR) spectrum is generally used for the determination of metal oxide bonds of ceramics [20]. The FTIR spectrum of barium titanate ceramics sintered at 800^{o}C is recorded in the range of 400-4000 cm^{-1} as shown in Fig.3 and showed metal oxide absorption bands at 489.9 cm^{-1} and 504.6 cm^{-1}corresponding to Zn-O and Ti-O, respectively [21, 22].

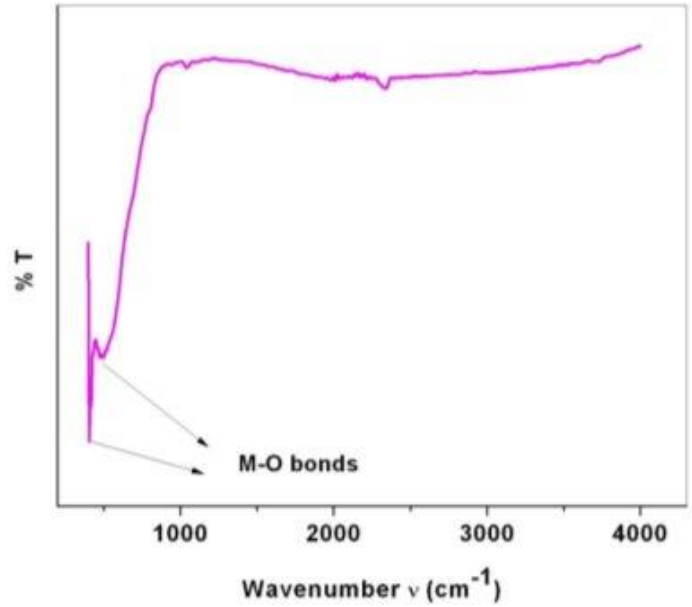

Figure 3*. FTIR spectrum of $ZnTiO_3$ ceramic.*

3.4. UV-Visible Spectrum

The diffuse reflectance spectrum (DRS) is recorded in the range of 200-1600 nm as depicted in Fig.4 for finding optical band gap energy of powder samples. Kubelka-Munk function of reflectance F(r) is used to determine band gap [23-25].

$$F(r) = \frac{(1-r)^2}{2r} \quad (3)$$

The maximum absorption wavelength is recorded to be 295 nm.

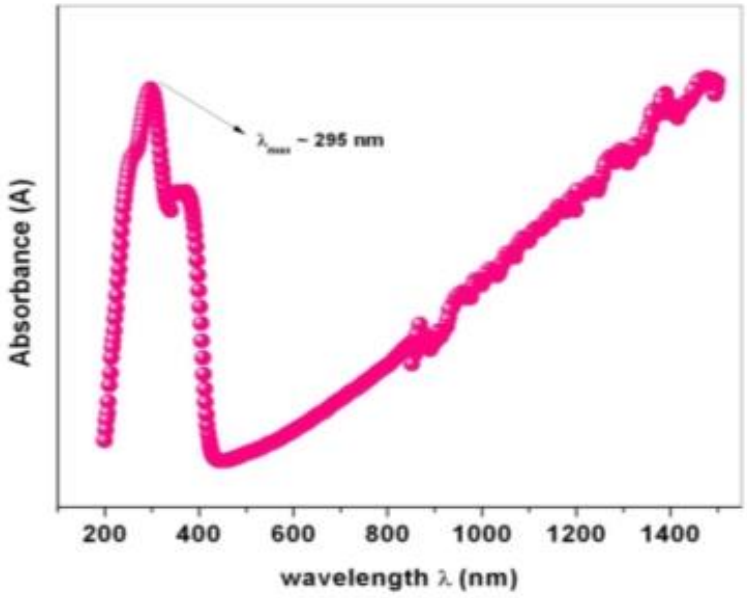

Figure 4. *The absorption spectrum of $ZnTiO_3$ ceramic.*

The absorption coefficient (α) is directly proportional to F(r) and hence an equation to find band gap can be written as follows [26-28].

$$(\alpha h\nu)^n = m\,(h\nu - E_g) \quad (4)$$

Where, m= Energy- independent constant that depends on transition probability, E_g= optical band gap energy, n= the kind of transition i.e. n = 2 for direct transition, 2/3 for direct forbidden transition, ½ for indirect transition, 1/3 for indirect forbidden transition and hν = photon energy [29]. In this study direct and indirect transitions are considered. E_{op} value is evaluated from the linear portion that is extrapolated towards X-axis for $(\alpha h\nu)^2$ versus photon energy hν(eV) plot as α tends to zero (Fig.5). The optical band gap energies for direct and indirect transitions are calculated as 3.03eV and 2.83eV, respectively.

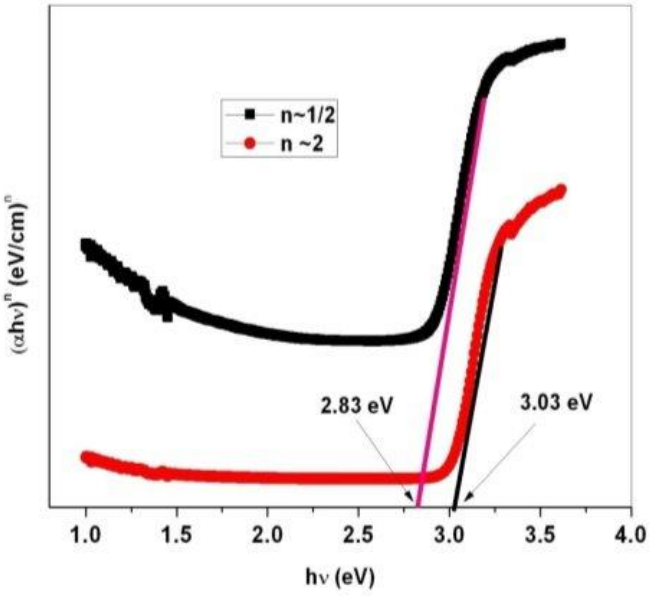

Figure 5. *The 'hν' versus '$(\alpha h\nu)^n$' plot of $ZnTiO_3$ ceramic.*

3.5. Dielectric Properties

The variation of dielectric constant (ε') and loss (ε") of $ZnTiO_3$is shown in Fig.6&7, respectively, as a function of both frequency (200 Hz-5 MHz) and temperature (313-673K). It can be seen from the figures, that the dielectric constant and loss is found to increase slowly with the increase of temperature up to 600 K and above 600K a sharp increasing trend in both the cases is observed. The constant variation of dielectric constant and loss was mainly attributed to theweak response of the charge carriers for the provided input temperature. For further increase of temperature the charge carriers will get activated and therefore they will be moved to the excited level which in turn leads to the enhancement of electrical properties.The sharp increase can be attributed to the interfacial or space-charge polarization effect [30, 31]. In addition, ε' and ε" were found to decrease with increase of frequency. This happens due to ineffective space-charges at the grain boundary interface. At room temperature, for f~ 5 MHz the present specimen showed dielectric constant of ~50. In general, the polarization due to grain boundaries are more active at the lower frequencies, and as the frequency increase the polarization due to grains will be more. Up to 100 Hz frequency, the space-charge or Maxwell-Wagner interfacial polarization becomes predominant and for further increase of frequency, the effectiveness of space-charges will be diminished. Thus, the dielectric constant as well as loss will be decreased.The transition temperature is noticed at ~663 K at which the structural transformation usually occurs. Normally, at the transition temperature all the charge carriers will be accumulated at the grain boundary interface and therefore the resistivity of the grain

boundary decreases. Hence, the breakage of grain boundary takes place which can again responsible for the peak value of dielectric constant or loss. At this juncture the entropy may be in general found to be very high. After transition temperature, the charge carriers will gradually come to the normal position. That is, the relaxation of charges may take place. In addition, the dielectric constant and loss plots (temperature dependent plots) reveal the distortion behavior at few temperatures. This can be attributed the presence of defect centers, strain variation, grain size variation etc. In other words, the imperfections will work as scattering centers to the charge carriers and hence the huge value of dielectric constant or loss may be obtained.The loss was also showing the similar trend as that of permittivity in all respects. This kind of high ε' and high ε" values noticed at room temperature are most suitable for filter, charge stored capacitors and absorber applications [32].

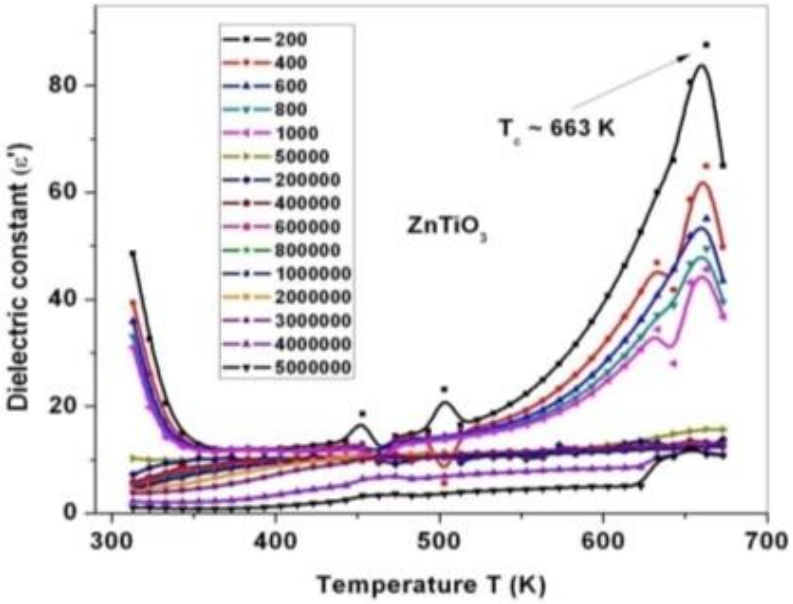

Figure 6. *The variation of dielectric constant (ε') with temperature.*

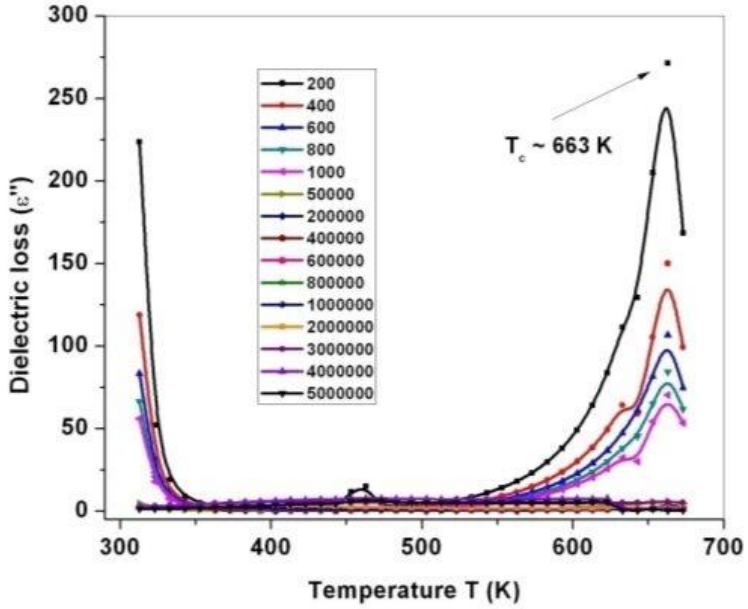

Figure 7. *The variation of dielectric loss (ε") with temperature.*

Figure 8 shows the variation of ac conductivity as a function of reciprocal of temperature at different frequencies (400 Hz- 3 MHz). As the temperature increases , the ac- conductivity increases owing to the hopping of charge carriers and hence this can be governed by the Arrhenius equation [33]:

$$\sigma_{ac} = \sigma_0 \exp\left(\frac{-Ea}{KT}\right) \quad (5)$$

where, $K=8.6\times10^{-5}$eV, σ_0= pre exponential factor, and T= absolute temperature.

In general, σ_{ac} can be calculated using the equation [34]: $\sigma_{ac}=\varepsilon_0\varepsilon_r\omega \tan\delta$, where ε_r =dielectric constant, $\varepsilon_0=8.9 \times 10^{-12}$ F/m, $\omega=2\pi f$ and tanδ= loss tangent. The $\ln\sigma_{ac}$ and 1000/T plots almost show a curve shape. The intersecting point of these two curves in general termed as the transition point [35]. Two slopes were taken on either side of curves as shown in plots. Normally, above the transition temperature, a definite change of conductivity is observed. These two slopes provide two activation energies i.e. 0.125 and 0.418 eV. The smaller activation energy was noticed in the high temperature region (>384 K) while higher activation energy is observed in the low temperature region (<384 K). This kind of variation of activation energy was mainly due to the conductivity behavior at lower and higher temperatures. Similar kinds of observations were made by Naidu et al. [35].

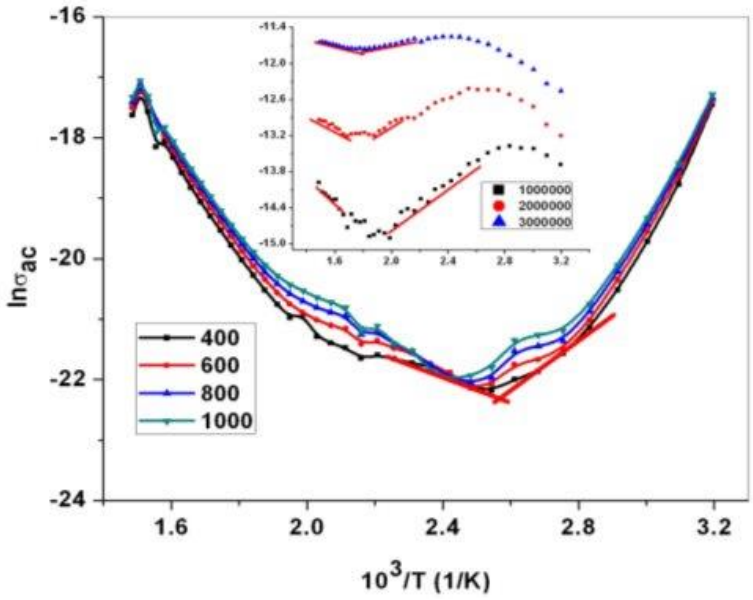

Figure 8. *The $\ln\sigma_{ac}$ and 1000/T plots of $ZnTiO_3$ ceramic.*

The frequency dependence of ac conductivity was depicted in Fig.9. It is noticed that the conductivity was increasing with frequency. This variation can be governed by the power law relation [**35-37**]: $\sigma_{ac}(\omega, T) = \sigma_o(T) + A\omega^n(\omega)$, where A is constants and n is exponent(varying between 0 -1). The term σ_o (T) indicates the dc-conductivity which is independent of frequency. The power law fit revealed the dc-conductivity of 2.20×10^{-8} S/cm at room temperature (313 K).The σ_o is varying between 2.20×10^{-8} - 1.18×10^{-10} S/cm. The exponent values were increasing with temperature from 0.24-0.67. This confirmed that the 'n' value was greater than zero and less than one. Within the frequency independent region or DC-conductivity region 'n' becomes zero, whereas the same showed greater than one, when the correlated barrier hopping (CBH) conduction mechanism took place in the sample as a function of frequency due to translation motion of charges. Hence, it was confirmed

that the electrical hopping type of conduction mechanism was accomplished in the present materials [**36, 37**].

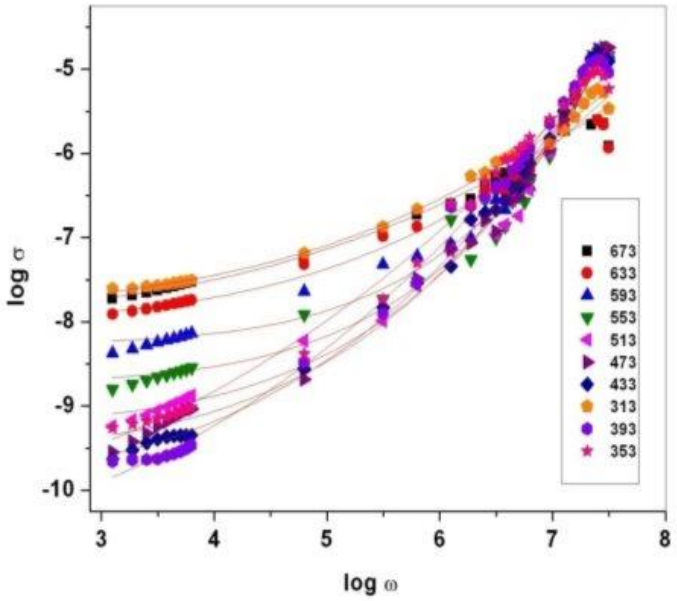

Figure 9. *Thelogσversus frequency plots of $ZnTiO_3$ ceramic.*

4. Conclusions

The zinc titanate (ZT) ceramic material is synthesized via conventional solid state reaction method. The rhombohedral structure is confirmed form diffraction study. A high optical band gap of 3.03eV is attributed to ZT when a direct transition is considered. However, these kinds of materials comprising wide optical band gaps can provide applications in optoelectronic devices, photo catalytic and sensor devices.The SEM micrographs confirmed the formation of almost spherical shape grains. In addition, the average grain size was noted to be approximately 720 nm.The obtained high permittivity and loss values provide dielectric absorber and charge stored capacitor applications. The two kinds of activation energies on either side of Arrhenius plots were seen which may be attributed to the change of slope and gradient line before and after transition temperature.The power law fit revealed the dc-conductivity of 2.20×10^{-8} S/cm at room temperature (313 K). Further, the exponent values were increasing with temperature from 0.24-0.67. The exponent value achieved less than unity indicated the existence of hopping conduction mechanism among the charge carriers.

Conflicts of Interest

The authors declare that there is no conflict of interest regarding the publication of this article.

Acknowledgments

I acknowledge to Vellore Institute of Technology (VIT), Tamilnadu for providing XRD facility. In addition, we are very much thankful to Mr. Sathish Kumar for helping characterization works in time. Also, thankful to Gurulinga from IISC-Bangalore, Karnataka for helping SEM characterization and analysis of morphology of the present materials.

References

[1] Abdelrahman A.; Badawy; Shaymaa E.; El-Shafey; Suzan Abd El All; Gamil A. El Shobaky. Effect of γ-Irradiation and Calcination Temperature of NanosizedZnO/TiO_2 System on its Structural and Electrical Properties. *Advances in Chemistry* 2014, 2014,1-7,Id:301410, DOI: http://dx.doi.org/10.1155/2014/301410.

[2] H. Obayashi, Y. Sakurai, T. Gejo, Perovskite-type oxides as ethanol sensors. *Journal of Solid State Chemistry* 1976, 17, 299-303, DOI: https://doi.org/10.1016/0022-4596(76)90135-3.

[3] Youichi Shimizu, HirokiKomatsu,SatokoMichishita,Norio Miura,Noboru Yamazo,Sensing characteristics of hydrogen peroxide sensor using carbon-based electrode loaded with perovskite-type oxide. *Sensors and Actuators* B, 1996, 34, 493-498, DOI: https://doi.org/10.1016/S0925-4005(97)80021-4.

[4] S. F. Wang, M. K. Lu, G. J. Zhou, Luminescent properties of Mn^{2+}-doped SnO_2 nanoparticles. *Inorganic Chemistry Communication* 2003, 6, 882-885, DOI: https://doi.org/10.1016/S1387-7003(03)00135-7.

[5] M. Skoglundh,L.O. Löwendahl,J.-E. Otterated,Combinations of platinum and palladium on alumina supports as oxidation catalysts. *Applied Catalyst,* 1991, 77, 9-20, DOI: https://doi.org/10.1016/0166-9834(91)80019-S.

[6] Y. S. Chang, Y. H. Chang, G. J. Chen,Synthesis and characterization of zinc titanate doped with magnesium. *Solid State Communications,* 2003, 128, 203-208, DOI: https://doi.org/10.1016/S0038-1098(03)00527-1.

[7] 7. Y. Gui, S. Li, J. Xu, Study on TiO_2-doped ZnO thick film gas sensors enhanced by UV light at room temperature. *Microelectronics Journal,* 2008, 39, 1120-1125, DOI: https://doi.org/10.1016/j.mejo.2008.01.05.

[8] S. F. Wang, F. Gu, M. K. Lu, D. R. Yuan, Photoluminescence of sol–gel derived $ZnTiO_3$:Ni^{2+} Nanocrystals. *Chemistry Physics Letters*, 2003, 373, 223-227, DOI: https://doi.org/10.1016/S0009-2614(03)00620-1.

[9] BudigiLokesh, S. Kaleemulla, and N. MadhusudhanaRao, Synthesis and Characterization of Zinc titanates by Solid state reaction. *International Journal of ChemTech Research*,2014, 6, 1929-1932. Available online: http://sphinxsai.com/2014/vol6pt3/12/(1929-1932)_ICMCT14.pdf (accessed on 23 April 2017).

[10] K. Chandra Babu Naidu, T. SofiSarmash, M. Maddaiah, P. Sreenivasula Reddy, D. Jhansi Rani and T. Subbarao, Synthesis and Characterization of MgO- doped $SrTiO_3$ Ceramics. *Journal of The Australian Ceramic Society*, 2016, 52, 95-101. Available online: http://austceram.com/volume-52-number-1-2016/ (accessed on 23 April 2017).

[11] E. Elayaperumal, Girish M. Joshi and M. Malathi, Structural and Dielectric Studies of CuO doped Sr2Bi4Ti5O18 Ferroelectric Ceramics. *International Journal of ChemTech Research*,2014-2015, 7, 212-217. Available online: http://sphinxsai.com/2015/ch_vol7_no1/3/(212-217)%20014.pdf (accessed on 23 April 2017).

[12] A.Vanaja, G.V.Ramaraju and K.SrinivasaRao, Influence of Copper doping on Structural, Morphological and Optical Properties of ZnO Nanoparticles.

International Journal of ChemTech Research,2015, 8, 703-710. Available online: http://sphinxsai.com/2015/ch_vol8_no12/3/(703-710)V8N12CT.pdf (accessed on 23 April 2017).

[13] S.Vadivelan, N.VictorJaya, Investigation of Structural, Thermal and Magnetic propertiesof Strontium substituted Barium Hexaferrite Synthesized via co-precipitation Method. *International Journal of ChemTech Research*, 2015, 8, 404-410. Available online: http://sphinxsai.com/2015/ch_vol8_no12/2/(404-410)V8N12CT.pdf (accessed on 23 April 2017).

[14] D Jhansi Rani, A Guru Sampath Kumar, T SofiSarmash, K Chandra Babu Naidu, M. Maddaiah, T SubbaRao, Effect of Argon/Oxygen Flow Rate on DC Magnetron Sputtered Nano Crystalline Zirconium Titanate Thin Films. *Journal of the Minerals, Metals and Materials Society*, 2016, 68, 1647-1652. Available online: https://link.springer.com/article/10.1007/s11837-016-1910-5 (accessed on 23 April 2017).

[15] V. Narasimha Reddy, K. Chandra Babu Naidu, T. SubbaRao, Structural, Optical and Ferroelectric Properties of $BaTiO_3$ Ceramics. *Journal of Ovonic Research*, 2016, 12, 185- 191. Available online: http://www.chalcogen.ro/185_NarashimhaR.pdf (accessed on 23 April 2017).

[16] K. C. B. Naidu, V. N. Reddy, T. S. Sarmash, D. Kothandan, T. Subbarao, N. S. Kumar, Structural, morphological, electrical, impedance and ferroelectric properties of BaO-ZnO-TiO_2 ternary system. *J Aust Ceram Soc*, 2018. Available online: https://doi.org/10.1007/s41779-018-0225-0 (accessed on 23 April 2017).

[17] N. S. Kumar, R. P. Suvarna and K. C. B. Naidu, Sol-Gel Synthesized and Microwave Heated $Pb_{0.8-y}La_yCo_{0.2}TiO_3$ (y=0.2–0.8) Nanoparticles: Structural, Morphological and Dielectric Properties. *Ceramics International*, 2018, DOI: https://doi.org/10.1016/j.ceramint.2018.07.027.

[18] K. C. B. Naidu, T. S.Sarmash, V. N. Reddy, M. Maddaiah, P. Sreenivasula Reddy and T. Subbarao, Structural, Dielectric and Electrical Properties of La_2O_3 Doped $SrTiO_3$ Ceramics. *Journal of The Australian Ceramic Society*, 2015, 51, 94 – 102. Available online: http://austceram.com/volume-51-number-1-2015/ (accessed on 23 April 2017).

[19] S. Anil Kumar, K. Chandra Babu Naidu, Structural and Dielectric Properties of Bi_2O_3doped $SrTiO_3$ Ceramics. *International Journal of ChemTech Research*, 2016, 9, 58-63.
Available online: http://www.sphinxsai.com/2016/ch_vol9_no1/1/(58-63)V9N1CT.pdf (accessed on 23 April 2017).

[20] N. S. Kumar, R. P. Suvarnaand, K.C. B. Naidu, Phase Change and Ferroelectric Nature of Microwave Heated Lead Cobalt Titanate Nanoparticles Prepared by Sol-Gel Method. *International Journal of Applied Ceramic Technology*, 2018, 1-8, DOI: 10.1111/ijac.13056.

[21] M.A.F.de Souza, R.A.Candeia, A.C.Chaves, S.J.G.Lima, E.Longo, L.E.B.Soledade, I.M.G.Santos, A.G. Souza, Synthesis and Characterization of $Sr_{1-x}Mg_xTiO_3$ Obtained by the Polymeric Precursor Method. *Materials Letters*, 2005, 59, 549-553, DOI: https://doi.org/10.1016/j.matlet.2004.10.014.

[22] Roberto Koferstein, Till Walther, Dietrich Hesse, Stefan G Ebbinghaus, Preparationand characterization of nanosized magnesium ferrite powders by a

starch-gel processand corresponding ceramics, *Journal of Material Science*, 2013, 48, 6509-651.
Available online: https://link.springer.com/article/10.1007/s10853-013-7447-x (accessed on 23 April 2017).

[23] D. Kothandan, R. Jeevan Kumar, Optical Properties of Rare Earth Doped Borate Glasses. *International Journal of ChemTech Research*, 2015, 8, 310-314. Available online: http://www.sphinxsai.com/2015/ch_vol8_no6/1/(310-314)V8N6CT.pdf (accessed on 23 April 2017).

[24] P.Malarkodi1, J.C. Kannan, Structural and optical properties of $Zn_xCd_{1-x}O$ nanoparticles. *International Journal of ChemTech Research*, 2015, 8, 522-529. Available online: http://sphinxsai.com/2015/ch_vol8_no12/abstracts/A(522-529)V8N12CT.pdf (accessed on 23 April 2017).

[25] SavithaElango, KalainathanSivaperuman, Sol-Gel mediated synthesis of tri-doped TiO2 Nanoparticles towards application of photo catalysis and its kinetic study. *International Journal of ChemTech Research*, 2015, 8, 588-597. Available online: http://sphinxsai.com/2015/ch_vol8_no12/abstracts/A(588-597)V8N12CT.pdf (accessed on 23 April 2017).

[26] A.Kiruthiga and T.Krishnakumar, Synthesis and Characterization of Microwave-assisted ZnO Nanostructures. *International Journal of ChemTech Research*, 2015, 8, 104-110.
Available online: http://www.sphinxsai.com/2015/ch_vol8_no7/1/(104-110)V8N7CT.pdf (accessed on 23 April 2017).

[27] D Kothandan, R. Jeevan Kumar, Investigations on Electrical and Thermal Properties of Rare Earth Doped BiZnSr Borate Glasses. *Journal of The Australian Ceramic Society*,2016, 52, 156-166. Available online: http://austceram.com/volume-52-number-1-2016/ (accessed on 23 April 2017).

[28] Supriyono, YuniKrisyuningsihKrisnandi, and JarnuziGunlazuardi, Band Gap Energy Modification of TiO_2photo-electrode by PbS/CdS Quantum Dot to Enhance Visible Region Photocurrent. *International Journal of ChemTech Research*, 2016, 9, 191-198. Available online: http://sphinxsai.com/2016/ch_vol9_no7/1/(191-198)V9N7CT.pdf (accessed on 23 April 2017).

[29] K. Chandra Babu Naidu, T. SofiSarmash, M.Maddaiah, V.Narasimha Reddy and T.Subbarao. *AIP Conference Proceedings*, 2015, 1665, 040001-3, DOI: 10.1063/1.4917614.

[30] K. C. Babu Naidu, T.SofiSarmash, M. Maddaiah, A. Gurusampath Kumar, D. Jhansi Rani, V.SharonSamyuktha, L. Obulapathi, T.Subbarao, Structural and Electrical Properties of PbO - doped $SrTiO_3$ Ceramics. *Journal of Ovonic Research*, 11(2015), 79-84. Available online: http://www.chalcogen.ro/79_Naidu.pdf (accessed on 23 April 2017).

[31] M.Vasubabu, C.Sureshbabu, R.Jeevan Kumar, Studies on dielectric behaviour of Myrtaceace and Mimosoideae family Indian wood species. *International Journal of ChemTech Research*, 2016, 9, 80-84. Available online: http://www.sphinxsai.com/2016/ch_vol9_no2/abstracts/A(80-84)V9N2CT.pdf (accessed on 23 April 2017).

[32] D.ArulAsir Abraham, U.Sankar, S.Perumal, P.Selvarajan, Growth, Mechanical, Electrical, Optical, and Thermal properties of γ- Glycine crystal Grown using the AqueousSolution of α-Glycine and Guanidine Hydrochloride. *International Journal of ChemTech Research*, 2015, 8, 444-456. Available online: http://sphinxsai.com/2015/ch_vol8_no7/3/(444-456)V8N7CT.pdf (accessed on 23 April 2017).

[33] M.Maddaiah, K.ChandraBabu Naidu, D. Jhansi Rani, T. Subbarao, Synthesis and Characterization of CuO-Doped $SrTiO_3$ Ceramics. *Journal of Ovonic Research*, 2015, 11, 99-106. Available online: http://www.chalcogen.ro/99_Naidu.pdf (accessed on 23 April 2017).

[34] M. Maddaiah, A. Guru Sampath Kumar, L. Obulapathi, T. SofiSarmash, K. Chandra Babu Naidu, D. Jhansi Rani, T. SubbaRao, Synthesis and Characterization of Strontium doped Zinc Manganese Titanate Ceramics. *Digest Journal of Nano materials and Biostructures*, 2015, 10, 155-159. Available online: http://www.chalcogen.ro/155_Maddaiah.pdf (accessed on 23 April 2017).

[35] D. S. Kumar, K. C. B. Naidu, M. M. Rafi, K. P. Nazeer, A. A. Begam, G. R. Kumar, Structural and dielectric properties of superparamagnetic iron oxide nanoparticles (SPIONs) stabilized by sugar solutions. *Materials Science-Poland*, 2018, 36, 123-133, DOI: 10.1515/msp-2018-0017.

[36] D. Sivakumar, K. C. B. Naidu, K. P. Nazeer,M. M. Rafi,G. Rameshkumar, B. Sathyaseelan, G. Killivalavan, A. A. Begam, Structural Characterization and dielectric properties of Superparamagnetic Iron oxide nanoparticles. *Journal of the Korean Ceramic Society*, 2018, 55, 230-238. Available online: https://www.jkcs.or.kr/journal/view.php?number=8118 (accessed on 23 April 2017).

[37] N. S. Kumar, R. P. Suvarna, K. C. B. Naidu, G. R. Kumar, S. Ramesh, Structural and functional properties of sol-gel synthesized and microwave heated $Pb_{0.8}Co_{0.2-z}La_zTiO_3$ (z = 0.05–0.2) nanoparticles. *Ceramics International*, 2018, DOI: https://doi.org/10.1016/j.ceramint.2018.07.176.